External Control of a Metal-Insulator Transition in (Ga,Mn)As Wires

Anh Kiet Nguyen and Arne Brataas
Department of Physics, Norwegian University of Science and Technology, NO-7491, Trondheim, Norway.

Quantum transport in disordered ferromagnetic (III,Mn)V semiconductors is studied theoretically. Mesoscopic wires exhibit an Anderson disorder-induced metal-insulator transition that can be controlled by a weak external magnetic field. This metal-insulator transition should also occur in other materials with large anisotropic magneto resistance effects. The transition can be useful for studies of zero-temperature quantum critical phase transitions and fundamental material properties.

The metal-insulator transition (MIT), a zero-temperature quantum phase transition, has since the beginning of the 20$^{\text{th}}$ century attracted much research interest [1, 2]. The MIT is conventionally driven by temperature, pressure, voltage, doping, and magnetic field amplitude [1, 2]. Examples of systems with MIT induced by external stress are the doped semiconductors Si:P and Si:B [3]. Despite considerable efforts, there are still controversies on fundamental issues such as critical exponents, universality classes, and scaling functions for the MIT in many systems [1, 2, 3]. Systems with new non-destructive external knobs that continuously control the metal-insulator transition are of great interest and can provide new insights on zero-temperature quantum phase transitions. For example, the determined critical exponents applies for all other systems in the same universality class. Furthermore, deviations between theoretical and experimental extracted critical exponents can indicate the carrier interaction strength [4].

We show that mesoscopic wires with a large anisotropic magneto resistance (AMR) effect [5] can undergo an Anderson metal-insulator transition driven by the magnetization *direction* which may be controlled by a weak external magnetic field. This is a new way to externally control a MIT. In systems with large AMR, the elastic mean free path (l) strongly depends on the magnetization direction (θ). Since the localization length (ξ) depends on l [6], it also exhibits a strong magnetization direction dependence. Additionally, quantum confinement can enhance the θ dependence of ξ. In mesoscopic quantum wires with large AMR, there can be a magnetization direction (θ_i) where the localization length is shorter than the phase coherence length (L_ϕ) leading to insulating behavior. For another magnetization direction (θ_m), the localization length can be longer than the phase coherence length L_ϕ giving a metallic behavior. Between those two magnetization directions there is an *Anderson disorder-induced, metal-insulator transition* [4].

Let us crudely estimate the required material parameters for observing the AMR-driven MIT. For diffusive quantum wires, the conductance is $G \simeq G_{\text{Sh}} l/(l + L_y)$ where G_{Sh} is the Sharvin conductance and L_y is the wire length [6]. The wire becomes localized when $G \sim e^2/h$, thus $\xi \sim l G_{\text{Sh}} h/e^2$ [6]. Consequently, the ratio between the localization lengths for two different magnetization directions is $\xi(\theta_i)/\xi(\theta_m) \sim G_{\text{Sh}}(\theta_i) l(\theta_i)/G_{\text{Sh}}(\theta_m) l(\theta_m)$. Now, consider a quantum wire long enough so that transport is localized for all magnetization directions. Here, $R(\theta) \sim e^{L_y/\xi(\theta)}$ so that the AMR resistance ratio becomes $R(\theta_i)/R(\theta_m) \sim e^{L_y(\xi_m - \xi_i)/(\xi_m \xi_i)}$, where $\xi_i = \xi(\theta_i)$. The maximum AMR ratio is achieved when L_y approaches the longest localization length ξ_m making the wire metallic for θ_m while still localized for θ_i. In this case, roughly, $R(\theta_i)/R(\theta_m) \sim e^{\xi_m/\xi_i - 1}$. Assume that a resistance ratio around 5 is sufficient for observing the MIT experimentally. This requires a diffusive AMR ratio $l(\theta_i)/l(\theta_m) \sim 0.6$ and a Sharvin AMR ratio $G_{\text{Sh}}(\theta_i)/G_{\text{Sh}}(\theta_m) \sim 0.6$. Therefore, ferromagnetic wires close to the insulating phase with AMR effects around 40% or larger are good candidates for observing the MIT at low temperatures. It is easy to experimentally demonstrate that such a colossal magnetoresistance effect arises from the MIT because of its extreme temperature sensitivity. The temperature dependence of resistance and conductance fluctuations may also be used to extract the phase coherence length and its temperature dependence.

This low temperature metal-insulator transition will not occur in the conventional ferromagnets Fe, Ni, and Co. The spin-orbit interaction is weak and the AMR effect is only a couple of percent. Furthermore, Fe, Ni, and Co are good metals, $k_F l \gg 1$, and the Fermi wavelength ($2\pi/k_F$) is on the sub-nanometer scale so even nano-scale confinement will not drive the system to the insulating phase. Novel ferromagnetic materials are required.

We use mesoscopic wires of ferromagnetic (III,Mn)V semiconductors (DMS) to demonstrate the idea. Four features make DMS suitable: 1) The mean free path strongly depends on the magnetization direction [5]. 2) State-of-the art ferromagnetic (III,Mn)V semiconductors are dirty and poor metals with $k_F l \sim 1$ [7], even bulk DMS are close to the insulating state. 3) The Fermi wavelength is very long ($\sim 5nm$) enabling the production of quantum wires with few transverse modes for rather modest constriction sizes. 4) The charge carrier concentration can be controlled by a gate potential. This may be used to decrease the Fermi energy (E_F) and increase the Fermi wavelength, i.e. reducing $k_F l$ and enhancing effects of quantum confinement. Both effects drive the system closer to the insulating phase.

Localization requires the localization length to be sig-

nificantly shorter than the phase coherence length which has been measured in (Ga,Mn)As and (In,Mn)As to be $\sim(50,100,200)nm$ at temperatures $\sim(2000,100,20)mK$, respectively [8]. We show below that for clean, $k_F l\sim 10$, (Ga,Mn)As wires clear signatures of the metal-insulator transition are observed for $L_\phi \sim 400nm$. Typical ferromagnetic (III,Mn)V semiconductors are much dirtier, $k_F l \sim 1$, than our simulations [9]. In these samples, $L_\phi \sim 50nm$ should be sufficient to observe the reported metal-insulator transition. The MIT we predict should, therefore, be observable with state-of-the art DMS. Scaling relations for a critical MIT gave good fits to measured resistivities as functions of temperature and magnetic field in DMS [7]. This further support the existence of a MIT in ferromagnetic (III,Mn)V semiconductors.

Critical phase transitions occur only in the thermodynamic limit. In finite systems, when the coherence length of critical fluctuations approaches the system size, finite size effects set in and prevent further development of singular behaviors [10]. In this sense, the metal-insulator transition we report is a *cross-over*. However, the phase coherence length and the localization length may be externally controlled by temperature and a gate potential. Thus, for a given set of material parameters, one may tune L_ϕ and ξ such that the condition $\xi_{\theta_i} \ll L_\phi \leq \xi_{\theta_m}$ is satisfied and a MIT may be studied within the finite size limitation [10].

Magnetization controlled metal-insulator switching in (Ga,Mn)As tunnel junctions have recently been observed in experiments [11]. The switching was interpreted to result from the magnetization-direction dependent hole-bound-states in a thin depleted (Ga,Mn)As layer in contact with a tunnel junction or a constriction [11]. It is easy to distinguish between such a scenario [11] and the MIT reported here using the conductance fluctuations which for a switching scenario [11] should be dominated by conventional bulk conductance fluctuations. In contrast, we report an Anderson disorder-induced quantum critical metal-insulator transition with the corresponding quantum critical fluctuations which strongly depends on the magnetization direction.

We capture the essential quantum transport properties of ferromagnetic (III,Mn)V semiconductors with a discrete Hamiltonian

$$H = (\gamma_1 + \frac{5}{2}\gamma_2)\frac{p^2}{2m_e} - \frac{\gamma_2}{m_e}(\mathbf{p}\cdot\mathbf{J})^2 + \mathbf{h}\cdot\mathbf{J} + V(\mathbf{r})\,. \quad (1)$$

Here, γ_1 and γ_2 are the Luttinger parameters [12], m_e is the electron mass, $\mathbf{J}$ is a vector of 4×4 spin matrices for J=3/2 spins, and $\mathbf{p}$ is the momentum operator in a finite difference form, e.g. $p_x^2 f(x_i) = -\hbar^2[f(x_{i+1}) - 2f(x_i) + f(x_{i-1})]/a_x^2$, where a_x is the lattice constant along x-axis. The first two terms in Eq.(1) is the 4×4 Luttinger Hamiltonian for zincblende semiconductors in the spherical approximation [13]. The third term in Eq.(1) describes the exchange interaction between itinerant holes and localized magnetic Mn dopants which are modeled by a mean-field, homogeneous exchange field $\mathbf{h}=J_{pd}N_{Mn}\mathbf{M}$, where J_{pd}, N_{Mn} and $\mathbf{M}$ are exchange interaction, volume density and average magnetic quantum number of the local Mn magnetic moments [14], respectively. A slightly more complicated 6 band version of Eq.(1) quantitatively explains many features of DMS [14].

Disorder is important in ferromagnetic (III,Mn)V semiconductors, but detailed knowledge of the impurity states and how they affect the transport properties are lacking [15]. The impurity types and configurations even depend on the annealing protocols [15]. We believe our band model with a short range Coulomb disorder potential provides a good starting point for theoretical studies of disorder effects on transport in ferromagnetic (III,Mn)V semiconductors. We use Anderson impurities, $V(\mathbf{r}) = \sum_i V_i\delta_{\mathbf{r}-\mathbf{R}_i}$, where V_i and $\mathbf{R}_i$ are the strength and the position of impurity number i and δ is the Kronecker delta. There is one impurity at each lattice site. The impurity strengths are randomly and uniformly distributed between $-V_0/2$ and $V_0/2$.

We consider the low temperature linear response transport regime. The conductance is calculated using the Landauer-Bütikker formula $G = \sum_{n,m}|t_{n,m}|^2e^2/h$, where $t_{n,m}$ is the transmission amplitude from transverse mode m to mode n at E_F. Due to quantum coherence, our system is not self-averaging. To study general features, we ensemble average over N_I=640 independent impurity configurations, e.g. $\langle G\rangle = \sum_{i=1}^{N_I} G_i/N_I$. The conductance fluctuation is defined as $\delta G = \sqrt{\langle G^2\rangle - \langle G\rangle^2}$ and the impurity-averaged resistance $\langle R\rangle = 1/\langle G\rangle$.

Our system is a discrete, disordered conductor sandwiched between two clean reservoirs with the same cross section. The transport direction is along the y-axis. The dimensions are $L_x = 36nm$, $L_y = [15 - 1500nm]$ and $L_z = 27nm$, comparable to recent experimental samples [8]. The spacings between the lattice points are a_x=a_y=a_z=$1.5nm$, much smaller than the typical Fermi wavelengths used $\lambda_F \sim 10nm$. The hole density is assumed to vanish outside the wire's cross section. We calculate the conductance numerically using a stable transfer matrix method [16, 17].

We consider homogeneous magnetizations in the z-y plane. The magnetization is parallel to the z-axis (wire) when θ=0 (θ=$\pi/2$). Special attention is on the directions: $\mathbf{h}_\perp \equiv h_0\hat{z}$, $\mathbf{h}_\angle \equiv h_0(\hat{z}+\hat{y})/\sqrt{2}$, and $\mathbf{h}_\parallel \equiv h_0\hat{y}$. The same subscripts are used for other quantities, e.g $\langle R_\perp\rangle$, $\langle R_\angle\rangle$, and $\langle R_\parallel\rangle$. We use the model parameters: $\gamma_1 = 7.0$, $\gamma_2 = 2.5$, $E_F = 0.03eV$, $h_0 = 0.06eV$ and $V_0 = 0.25eV$ [14]. Mesoscopic ferromagnetic (III,Mn)V semiconducting wires are generally expected to be partly depleted [18]. Hence, E_F should be significantly smaller than its bulk value $E_F \sim 0.1eV$. Furthermore, E_F may also be reduced by a gate potential. The impurity strength V_0=$0.25eV$ gives $l\sim20nm$ which correspond to

a clean system, $k_F l \sim 10$ [9].

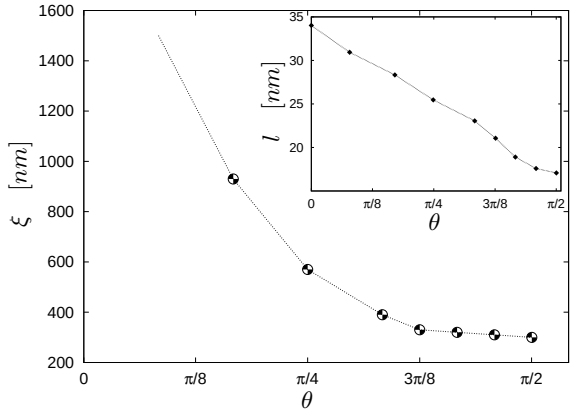

FIG. 1: Localization length versus magnetization direction. θ=0 (θ=$\pi/2$) is perpendicular (parallel) to the wire. Line is guide to the eye. Inset: Mean free path versus magnetization direction.

We estimate the mean free path by fitting the transmission probability $T = G/G_{\rm Sh}$ to $T(L_y) = l/(l+L_y)$ [6]. Fig. 1 inset shows the mean free path versus magnetization direction for a (Ga,Mn)As wire. We see that l decreases from $34nm$ to $17nm$ when the magnetization changes from perpendicular to parallel to the wire. We show below that this magnetization direction controlled reduction of the mean-free-path by a factor of two is sufficient to induce an observable metal-insulator transition.

The localization length is estimated using $\langle R\rangle \propto e^{-L_y/\xi}$ at large L_y. Fig. 1 shows that the localization length decreases strongly for increasing magnetization angle, with a minimum $\sim 300nm$ at θ=$\pi/2$. Note that $\xi(\theta)$ decreases several times stronger than $l(\theta)$ due to quantum confinement [6]. Thus, for a given impurity strength there exist a large range of wire lengths (or phase coherence lengths in the case $L_\phi < L_y$) where $\xi(\theta$=$\pi/2) \ll L_y \leq \xi(\theta$=$0)$, and a metal-insulator transition may be driven continuously by the magnetization direction.

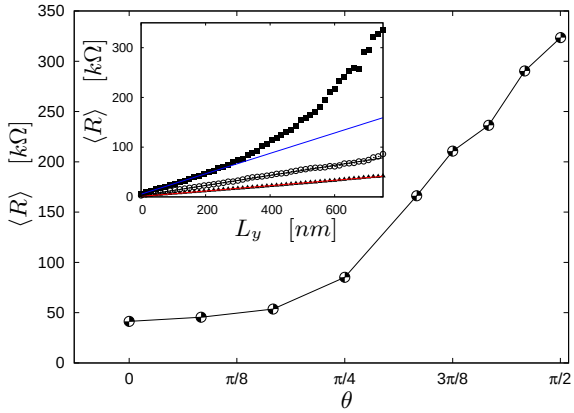

FIG. 2: Impurity averaged resistance versus magnetization angle for a wire with length L_y=$750nm$. Inset: Impurity-averaged resistance versus wire length for $\mathbf{h}_\perp$ (triangles), $\mathbf{h}_\angle$ (circles) and $\mathbf{h}_\parallel$ (squares). Linear lines are best fit to data at small L_y.

Fig. 2 inset shows impurity-averaged resistances versus wire length for the magnetizations $\mathbf{h}_\perp$, $\mathbf{h}_\angle$ and $\mathbf{h}_\parallel$. The transport is diffusive for $\mathbf{h}_\perp$ since $\langle R_\perp\rangle$ is linear for all wire lengths up to L_y=$750nm$. $\langle R_\angle\rangle$ shows weak non-linear behavior for $L_y > 600nm$. For $\langle R_\parallel\rangle$, a clear transition from linear to exponential behavior takes place around $L_y \sim 300nm$. Thus, the quantum wire is metallic for $\mathbf{h}_\perp$ and localized for $\mathbf{h}_\parallel$. Between those two extreme directions, there is *an Anderson disorder-induced metal-insulator transition which may be continuously controlled by the magnetization direction.*

Fig. 2 shows the impurity averaged resistance versus magnetization angle. We see a change in the behavior of $\langle R\rangle$ around $\theta = \pi/4$, after which the resistance increases strongly for increasing angle indicating the insulating phase. For the particular wire the resistance increases $\sim$700% when θ increases from 0 to $\pi/2$. Compared to our simulations, state-of-the art experimental samples are much dirtier with much shorter localization lengths so that the AMR should greatly increase and become a colossal anisotropy magneto resistance effect.

Note that the anisotropy relation $\langle R_\perp\rangle < \langle R_\parallel\rangle$ is tightly connected to the narrow wire geometry. In ferromagnetic (III,Mn)V semiconductor films and bulk systems, one finds experimentally the opposite AMR relation, $\langle R_\perp\rangle > \langle R_\parallel\rangle$ [5]. We have also considered a film shaped system with L_x=$60nm$ and L_z=$18nm$. All other parameters are the same as above. Here, we find $\langle R_\perp\rangle > \langle R_\parallel\rangle$, consistent with the experimental findings. The explanation is as follows. Due to the strong spin-orbit interaction, the Fermi surface for heavy holes is prolonged along the magnetization direction forcing the distribution of transverse (k_x, k_z) modes/transport channels to be highly anisotropic for $\mathbf{h} = \mathbf{h}_\perp$ [17]. For bulk and film geometries, this anisotropy increases the probability for back scattering and thereby increases the resistance, $\langle R_\perp\rangle$. On the other hand, $\mathbf{h} = \mathbf{h}_\parallel$ gives a dense and circular symmetric distribution of transverse (k_x, k_z) modes which in narrow wires leads to more confinement, i.e. stronger 1D character and consequently more back scattering and higher resistance, $\langle R_\parallel\rangle$.

Finally, we use the the conductance fluctuations to confirm the existence of a metal-insulator transition. For ballistic transport δG=0. In the transition between ballistic and diffusive transport δG has a peak above its universal value at $L_y \sim l$ [19]. In the diffusive regime, δG attains a universal value [20]. In the localized regime, $(\delta G)^2 \propto \langle G\rangle$ and, thus, decreases for increasing wire (or phase coherence length) [19]. Fig. 3 shows conductance fluctuations versus wire length for the magnetizations $\mathbf{h}_\perp$, $\mathbf{h}_\angle$ and $\mathbf{h}_\parallel$. Since the first shown value for δG is at L_y=$15nm$ comparable to the mean-free-path, we do not see the rise from $\delta G = 0$ expected for the $L_y = 0$ (ballistic) case. We see that δG for all magnetization directions has a peak around $L_y \sim l \sim 20nm$ before they decrease to the same universal value. Despite large differ-

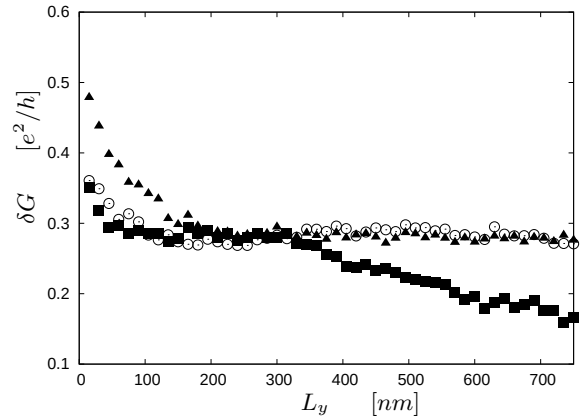

FIG. 3: Conductance fluctuations versus wire length for a (Ga,Mn)As wire with magnetizations $\mathbf{h}_\perp$ (triangles), $\mathbf{h}_\angle$ (circles) and $\mathbf{h}_\parallel$ (squares).

ences in the Sharvin resistances, conductances and mean-free-paths all magnetizations give, within numerical uncertainties, the same universal conductance fluctuations, $\delta G \approx 0.28e^2/h$. We see that the wire length must be ~ 10 times longer than the mean-free-path before the conductance fluctuation reaches its universal value. For $\mathbf{h}_\parallel$ and $L_y > 300nm$, the conductance fluctuation drops from its universal value and decreases for increasing wire length. This clearly indicates a localized phase where $\delta G \propto \sqrt{\langle G \rangle}$ [19], in agreement with single parameter scaling [21]. This drop in δG may be used to study the phase coherence length and its temperature dependence in the localized regime.

In conclusion, we have shown that (Ga,Mn)As mesoscopic wires of experimental sizes exhibit at mK temperatures an Anderson disorder-induced metal-insulator transition which may be continuously driven by the magnetization direction, which is a new way to control a MIT. This metal-insulator transition may be useful for studies of zero-temperature quantum critical phase transitions and fundamental properties of ferromagnetic (III,Mn)V semiconductors. The universal conductance fluctuations of (Ga,Mn)As wires are found to be independent of the magnetization direction, $\delta G \approx 0.28e^2/h$.

We thank S. Girvin, C. Gould, A. H. MacDonald, L. W. Molenkamp, A. Sudbø, Z. Tesanovic, C. Varma, and G. Zarand for stimulating discussions. This work has been supported by the Research Council of Norway through grant no. 162742/V00, 167498/V30, computing time through the Notur project and EC Contract IST-033749 "DynaMax".

[1] N. F. Mott, *Metal-Insulator transitions*, Taylor & Francis (London, 1990); *Metal-insulator transitions revisited*, Eds. P. P. Edwards and C. N. R. Rao, Taylor & Fransis (London, 1995).
[2] D. Belitz and T. R. Kirkpatrick, Rev. Mod. Phys. **66**, 261 (1994).
[3] M. A. Paalanen, T. F. Rosenbaum, G. A. Thomas and R. N. Bhatt, Phys. Rev. Lett. **48**, 1284 (1982); S. Bogdanovich, M. P. Sarachik and R. N. Bhatt, Phys. Rev. Lett. **82**, 137 (1999).
[4] P. W. Anderson, Phys. Rev. **109**, 1492 (1958); T. Giamarchi and H. J. Schulz, Phys. Rev. B **37**, 325 (1988).
[5] T. Hayashi *et al.*, Physica B **284**, 1175 (2000); D. V. Baxter *et al.*, Phys. Rev. B **65**, 212407 (2002); K. Y. Wang *et al.*, Phys. Rev. B **72**, 085201 (2005).
[6] D. J. Thouless, Phys. Rev. Lett. **39**, 1167 (1977); *Electronic Transport in Mesoscopic Systems*, S. Datta, Cambridge University Press (1995).
[7] G. Zaránd, C. P. Moca and B. Jankó, Phys. Rev. Lett. **94**, 247202 (2005); C. P. Moca *et al.*, arXiv:0705.2016 (2007).
[8] K. Wagner *et al.*, Phys. Rev. Lett. **97**, 056803 (2006); L. Vila *et al.*, Phys. Rev. Lett. **98**, 027204 (2007); A. Lee *et al.*, Appl. Phys. Lett. **90**, 032105 (2007).
[9] State-of-the-art experimental samples are in the dirty limit, $k_F l \sim 1$ which should make it easier to observe the MIT. However, proper modelings of these systems demand, at present, inaccessible computing power.
[10] *Finite size scaling and numerical simulation of statistical systems*, ed. V. Privman, World Scientific Publishing (1990).
[11] K. Pappert *et al.*, Phys. Rev. Lett. **97**, 186402 (2006); K. Pappert *et al.* Nature Physics **3**, 573 (2007).
[12] I. Vurgaftman, J. R. Meyer and L. R. Ram-Mohan, J. Appl. Phys. **89**, 5815 (2001).
[13] J. M. Luttinger, Phys. Rev. **102**, 1030 (1956); A. Baldereschi and N. O. Lipari, Phys. Rev. B **8**, 2697 (1973).
[14] T. Jungwirth *et al.*, Rev. Mod. Phys. **78**, 809 (2006); T. Dietl *et al.*, Science **287**, 1019 (2000); J. König *et al.*, in *Electronic Structure and Magnetism of Complex Materials*, edited by D. J. Singh and D. A. Papaconstantopoulos (Springer Verlag, 2002).
[15] C. Timm, J. Phys.: Condens. Matter **15** , R1865 (2003).
[16] T. Usuki *et al.*, Phys. Rev. B **52**, 8244 (1995).
[17] A. K. Nguyen, R. V. Shchelushkin and A. Brataas, Phys. Rev. Lett. **97**, 136603 (2006); A. K. Nguyen, H. J. Skadsem and A. Brataas, Phys. Rev. Lett. **98**, 146602 (2007).
[18] L. W. Molenkamp, private comunication.
[19] N. Giordano, Phys. Rev. B **38**, 4746 (1988); K. Tankei, M. Ikegami and Y. Nagaoka, J. Phys. Soc. Japan **63**, 1090 (1994).
[20] P. A. Lee and A. D. Stone, Phys. Rev. Lett. **55**, 1622 (1985); B. L. Al'tshuler and D. E. Khmel'nitshii, JETP Lett. **42**, 359 (1985).
[21] E. Abrahams, P. W. Anderson, D. C. Licciardello and T. V. Ramakrishnan, Phys. Rev. Lett. **42**, 673 (1979).